How the acoustic resonances of the subglottal tract affect the impedance spectrum measured through the lips

Noel Hanna,[a] John Smith, and Joe Wolfe
School of Physics, University of New South Wales, Sydney NSW 2052, Australia

(Received 19 January 2018; revised 27 March 2018; accepted 4 April 2018; published online 3 May 2018)

Experimental determinations of the acoustic properties of the subglottal airway, from the trachea below the larynx to the lungs, may provide useful information for detecting airway pathologies and aid in the understanding of vocal fold auto-oscillation. Here, minimally invasive, high precision impedance measurements are made through the lips (7 men, 3 women) over the range 14–4200 Hz during inspiration, expiration, and with a closed glottis. Closed glottis measurements show the expected resonances and anti-resonances of the supraglottal vocal tract. As the glottis is gradually opened, and the glottal inertance decreases, maxima in the subglottal impedance increasingly affect the measured impedance spectrum, producing additional pairs of maxima and minima. The pairs with the lowest frequency appear first. Measurements during a cycle of respiration show the disappearance and reappearance of these extrema. For a wide glottal opening during inspiration, and for the frequency range 14–4200 Hz, the impedance spectrum semi-quantitatively resembles that of a single, longer duct, open at the remote end, and whose total effective length is 37 ± 4 cm for men and 34 ± 3 cm for women. Fitting to simple models of the subglottal tract yields mean effective acoustic lengths of 19.5 cm for the men and 16.0 cm for the women in this study.
 https://doi.org/10.1121/1.5033330

[ZZ] Pages: 2639–2650

I. INTRODUCTION

The lower respiratory airway below the larynx, henceforth the subglottal tract, has important roles in both respiration and voice production. The relationship between pressure and flow is important in respiratory function, and low frequency measurements have been used diagnostically. During phonation, the vocal folds are acoustically loaded by two resonant ducts; the subglottal tract provides the upstream impedance and the supraglottal (vocal) tract provides the downstream impedance. The subglottal tract could thus significantly affect the auto-oscillation of the vocal folds that produces phonation.

Models of auto-oscillation usually include these two acoustic loads, and they suggest that, for instance, under some load conditions, upstream resonances should cause phonation instabilities. Such instabilities have been suggested to cause a global division of the vowel plane into front and back vowels, whose second formants tend to occur, respectively, above or below the second subglottal resonance Sg2 (Chi and Sonderegger, 2007; Lulich, 2010), where "resonance" in this context would mean an impedance maximum measured just below the glottis.[1] The challenge is that testing these models requires knowledge of the subglottal resonances.

Despite the inaccessibility of the larynx, some acoustic impedance measurements have yielded the frequencies of the impedance maxima of the subglottal tract at the glottis. van den Berg (1960) made swept sine acoustic impedance measurements on the lungs of human and canine cadavers and reported a subglottal resonance in humans at $f_{Sg1} \sim 300$ Hz, a value that has never been subsequently verified. The first *in vivo* measurements were made by Ishizaka *et al.* (1976) using swept sine excitation through the tracheostoma of laryngectomised male patients; they found subglottal impedance maxima Sgi at 640, 1400, and 2100 Hz with magnitudes ranging from 2.5 to 5 MPa s m^{-3}. Another approach involved analysing pressure signals above and below the glottis (Cranen and Boves, 1987), but this is complicated by the unknown spectrum of the vocal fold source.

More recently, accelerometers placed on the neck below the glottis have been used to monitor subglottal resonances during speech in order to discern their effect on the voice (e.g., Chi and Sonderegger, 2007; Lamarche and Ternström, 2008; Lulich, 2010; Zañartu *et al.*, 2011). It should be noted that the peaks in the spectral envelope of the acceleration measured at the skin contain unknown neck transfer functions, so while one would expect them to occur near peaks Sgi in the subglottal impedance, the relation may not be exact. Measurements made over wide frequency ranges have determined subglottal resonance frequencies f_{Sgi} close to the Ishizaka *et al.* (1976) values, i.e., resonances (impedance maxima at the glottis) at 640, 1400, and 2100 Hz for men (Lulich *et al.*, 2012), and 426, 1220, and 2000 Hz for a single tall male subject (Sundberg *et al.*, 2013).

Measuring the acoustic impedance of the entire airway from lips to lungs at very low frequencies, sometimes called the forced oscillation technique, has been explored for its potential clinical relevance to detecting lung pathologies (e.g., Campbell and Brown, 1963; Fredberg and Hoenig, 1978; Habib *et al.*, 1994; Harper *et al.*, 2001; Brown *et al.*, 2010; Robinson *et al.*, 2011) and the collapsibility of the airway, which is implicated as a cause of obstructive sleep apnea

[a]Electronic mail: n.hanna@unswalumni.com

(Smith *et al.*, 1988). These measurements are typically limited to a maximum of a few tens of hertz (Oostveen *et al.*, 2003).

More indirectly, the influence of the subglottal impedance has been observed as modifications in the speech pressure signal measured at the mouth when the average glottal aperture over the oscillation cycle is large, e.g., during breathy phonation (Fujimura and Lindqvist, 1971; Fant *et al.*, 1972; Stevens, 2000).

Zhang and colleagues (2006) showed that subglottal resonances can cause discontinuities in the frequency of oscillation (f_o) of a self-oscillating *in vitro* vocal fold model. However, instabilities caused by subglottal resonances are not always observed *in vivo*. For example, soprano singers can vary f_o smoothly across their first subglottal resonance Sg1 without showing systematic evidence of such instabilities (Titze *et al.*, 2008; Wade *et al.*, 2017). Similar studies with male singers also show little evidence for systematic instabilities at measured (Zañartu *et al.*, 2011) or expected subglottal resonance frequencies (Titze *et al.*, 2008).

The present study reports measurements of impedance spectra through the lips made during respiration using a technique previously demonstrated with a closed glottis (Hanna *et al.*, 2012) and during phonation (Hanna *et al.*, 2016a). This acoustic method can be conducted on healthy, normal subjects without discomfort or special preparation. The airway is excited by a signal injected through the lip aperture and measurements can therefore involve both the supraglottal (vocal) and subglottal tracts, when they are connected by the sufficiently low inertance associated with a relatively large glottal aperture. In the spirit of the simple models discussed in Sec. II, the results are compared with very simple duct models, and measurements on the same subjects with glottis closed are used for comparison.

II. THEORY

A. Models of the subglottal tract

Modeling the entire airway requires a satisfactory model of the human subglottal tract informed by its anatomy. Morphological data providing lengths and cross-sectional areas of the branches of the subglottal tract come from three main sources: Van den Berg's dissections of humans and canines (van den Berg, 1960), Weibel's (1963) measurements of excised lungs and casts, and Horsfield and colleagues who made measurements on casts of lungs (summarised in Horsfield *et al.*, 1971).

Models of the subglottal tract have sometimes used an electrical transmission line analogue to combine the available geometric and acoustic data. Such models are directly comparable to one-dimensional acoustic waveguides, which may have variations in the cross-sectional area of the waveguide along its length. In such models, reflections occur where there are changes in the total cross-sectional area of the airway. This means that the acoustic resonances depend primarily on the global area function (area as a function of distance from the glottis), rather than the dimensions of individual branches, which may not need to be treated individually. This neglect of topology is expected to underestimate wall losses. Such a simplification is shown in Fig. 1.

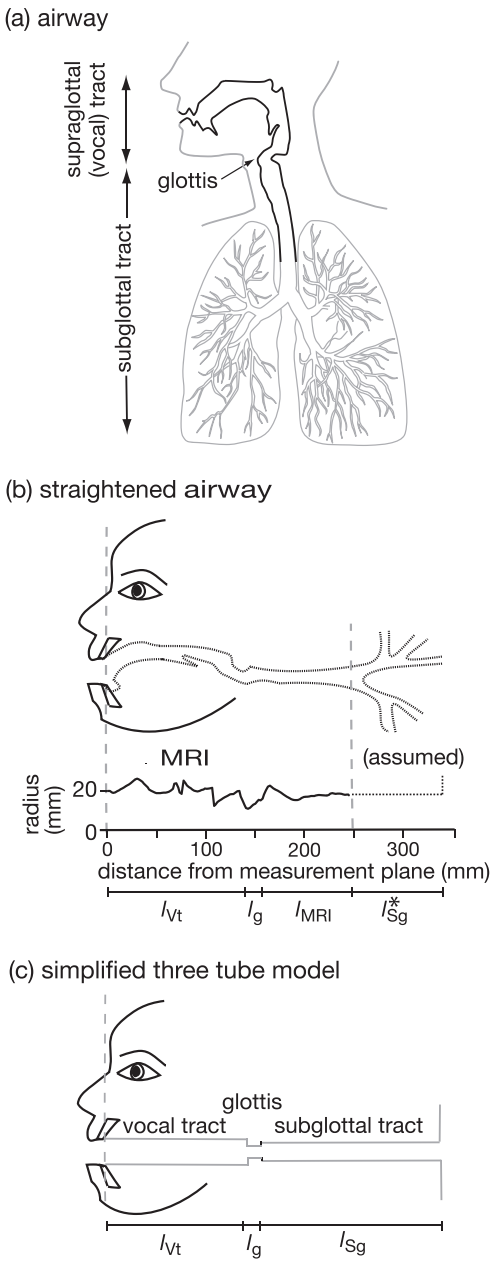

FIG. 1. Simplified anatomy of the respiratory airway showing (a) a sketch of the airway, (b) a straightened version of the tract and radius as a function of length from Hanna *et al.* (2016b), and (c) a simplified three tube version. The dashed vertical line common to (b) and (c) represents the measurement plane of the three-microphone impedance head.

It may seem surprising that there are few detailed geometric data available but most research into the subglottal airway is focused on respiration and hence the lower branches of the system that involve gas exchange, rather than the first few branching generations that are of greater importance to the acoustical response.

Because the cross-sectional area increases quickly with each generation of branches, the key features of the impedance are not strongly affected by including additional branching past about eight generations (Lulich, 2006). Hence it can be argued that the termination impedance of the alveolae need not be considered for acoustic measurements.

In an extreme simplification, Lulich *et al.* (2011) argue that the frequencies of the second and third subglottal

resonances are predicted approximately by treating the subglottal tract as an open cylinder (i.e., a one-dimensional waveguide terminated by a flanged radiation impedance) of acoustic length $l_{Sg} \sim 20$ cm. (More particularly, they suggest that the effective length is a person's height multiplied by 1/8.508, an empirically derived scaling factor). If the tract were terminated in this fashion, the ratios of the impedance maxima f_{Sg1}:f_{Sg2}:f_{Sg3} would be very close to 1:3:5, which substantially underestimates reported measurements of f_{Sg1}. However, non-rigid walls would raise the expected value of f_{Sg1}. Ishizaka and colleagues (1976) proposed an inertive wall impedance for this reason. Lulich and Arsikere (2015) attributed the difference mainly to the localised non-rigidity of the cartilage and tissue of the subglottal tract. Furthermore, the mechanical properties of the walls and the energy losses at the walls are expected to be important factors for determining the bandwidth of the resonances (Fredberg and Hoenig, 1978, Hanna *et al.*, 2016a).

B. A simple, rigid, symmetric model of the airway

Modeling how the subglottal resonances might affect the impedance measured through the lips (Z_{lip}) involves several complexities and effects that are best understood one at a time. For that reason, and to develop a nomenclature, the highly simplified three-tube model of the airway shown in Fig. 2 is used as a first idealisation. Impedance spectra are calculated with the glottis closed, fully open, and in three intermediate positions that might be representative of phonation and respiration. The subglottal tract is approximated using the model of Lulich *et al.* (2011): a rigid cylinder of length l_{Sg}, open at the remote end. For now, the supraglottal vocal tract is also approximated as a cylinder of length l_{Vt}—a reasonable approximation when the mouth is held in the position for the vowel /ɜ/ (Hanna *et al.*, 2016a). For this simple illustrative model, both the supra- and subglottal tracts are assumed to be rigid and have the same length (17 cm) and radius ($r_{Vt} = r_{Sg} = 1$ cm). The glottis that links them is approximated as a cylinder of effective length $l_g = 1$ cm and variable radius r_g. The impedance measured through the lips Z_{lip} can then be calculated using the transfer matrix method, with the open subglottal tract as a load at the remote end of the glottis and continuing to the lips. For all calculations in this paper, the complex attenuation coefficient α that accounts for wall losses is set at 5 times the value for visco-thermal losses in a smooth, rigid, cylindrical surface (Hanna *et al.*, 2016a).

With the glottis completely closed [Fig. 2(a)], the impedance minima (i.e., the resonances Ri when measured through the lips) are those of the supraglottal tract alone; a closed pipe with resonances around 500 Hz (R1), 1500 Hz (R2), 2500 Hz (R3), etc. (This is approximately what is observed for the vowel /ɜ/, with a closed or very small glottis and a relatively uniform supraglottal vocal tract cross section, as used in the current study.) The maxima $\bar{\text{R}}$i correspond to anti-resonances of the supraglottal tract. At the other extreme [Fig. 2(e)], a fully open glottis shows the impedance spectrum of an open pipe with slightly more than twice the length: it has minima around 500, 1000, 1500 Hz, etc. Compared with Fig. 2(a), the minima in Fig. 2(e) have approximately half the frequency spacing: there are twice as many of them.

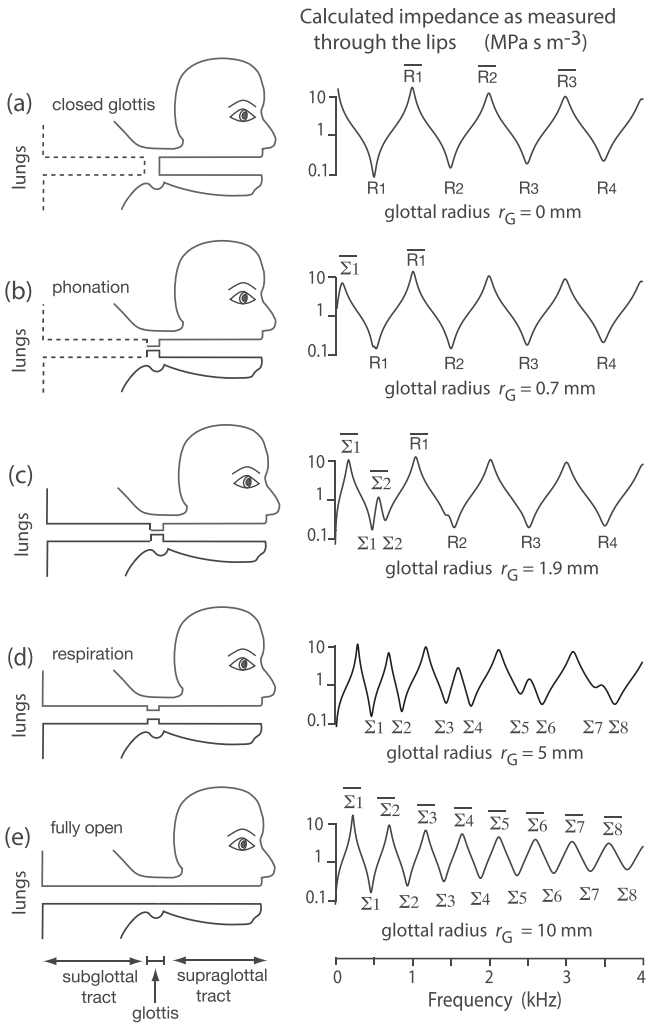

FIG. 2. A highly simplified, symmetric three-tube model of the airway (not to scale) with examples showing Z_{lip}, the calculated impedance magnitude through the lips, for different degrees of glottal opening. Calculations assumed $l_{Vt} = l_{Sg} = 17$ cm, $l_g = 1$ cm, $r_{Vt} = r_{Sg} = 1$ cm. For clarity only a few of the maxima have been labeled—see text for nomenclature.

Figure 2(b) shows the effect of slightly opening the glottis to a degree consistent with the average in normal phonation; the sub- and supraglottal tracts are now connected via the inertance of the glottis. This is still sufficiently large to isolate substantially the subglottal impedance from that of the supraglottal tract, consequently the impedance measured through the lips is almost unchanged, except for a slight perturbation of the first minimum around 500 Hz. Also, once the glottis is opened as in Fig. 2(b), the impedance at very low frequency must now drop to a low value as the rigid airway is no longer closed; consequently, a new impedance maximum $\bar{\Sigma}1$ appears below 100 Hz—see the next paragraph for explanation of the Σi nomenclature. Figure 2(c) shows a wider glottal opening whereby the sub- and supraglottal tracts are more effectively connected, introducing an additional minimum and maximum around 500 Hz. However, because inertance increases with increasing frequency, the sub- and supraglottal tracts are still not strongly connected at frequencies above 1 kHz in this case. Consequently, only a small perturbation is

apparent around the minimum R2. Figure 2(d) shows a glottal opening that might be consistent with respiration: the glottal inertance is now sufficiently low that the increasing influence of the subglottal tract can be seen in the introduction of additional maxima and minima extending up to 4 kHz. The glottal inertance thus plays a crucial role in determining the degree to which the subglottal impedance affects that measured through the lips.

How to name the resonances that substantially involve acoustic waves in both supra- and subglottal tracts? Assume that a measurement has been made with a closed glottis; the impedance minima and maxima at the lips are Ri and $\bar{\text{R}}$i, respectively. The nomenclature used here is that once the glottis is sufficiently open to show an additional minimum in impedance in the range near the first acoustic resonance of the supraglottal tract R1, these two minima be called Σ1 and Σ2 (Σ representing the combination or sum of the two tracts). Thus in Figs. 2(a) and 2(b), when the glottal inertance is high, all minima are called Ri. In Fig. 2(c), they are called Σ1, Σ2, R2, R3, and R4. In Fig. 2(d), Σ3 and Σ4 similarly replace R2, Σ5 and Σ6 replace R3, and Σ7 and Σ8 replace R4, so that Fig. 2(e) shows the Σi as resonances of an open tract with a total effective length $l_\Sigma = l_{\text{Vt}} + l_{\text{g}} + l_{\text{Sg}}$.

As for the impedance maxima, in the simple rigid model of Fig. 2(a) with closed glottis, it is clear that at low frequency the impedance should increase to be effectively infinite, so the first maximum at non-zero frequency occurs above f_{R1}, and is therefore an acoustic anti-resonance labeled $\bar{\text{R}}$1 (Hanna *et al.*, 2016a). Once the glottis is opened as in Fig. 2(b), the impedance at very low frequency of this simplified model must drop to a low value, so a new impedance maximum appears with a frequency that increases with decreasing glottal inertance to ∼250 Hz, the value expected for the first resonance of an open pipe with the length of the combined tracts, hence this impedance maximum is denoted by $\bar{\Sigma}$1.

C. A non-rigid asymmetric model of the airway

To examine this further, it is worthwhile considering a still simplified, but less symmetric situation, and including some wall properties. Figure 3 shows how the calculated maxima and minima measured through the lips change with increasing glottal radius r_{g} (i.e., with decreasing glottal inertance L_{g}). The situation considered now has different radii and lengths for each region ($l_{\text{Vt}} = 170$ mm, $r_{\text{Vt}} = 11$ mm, $l_{\text{g}} = 10$ mm, r_{g} variable, $l_{\text{Sg}} = 200$ mm, $r_{\text{Sg}} = 9.5$ mm). Furthermore, the supraglottal tract is now considered to have yielding walls; a uniformly distributed wall mass, spring constant, and loss are applied with parameters taken from Hanna *et al.* (2016a). A non-rigid tract closed at the glottis introduces a mechano-acoustic resonance R0 at ∼20 Hz due to the compliance and inertance of the surrounding tissues, and a mechano-acoustic anti-resonance $\bar{\text{R}}$0 at ∼200 Hz, due to the compliance of the air in the tract and the tissue inertance. Once the glottis is open, the resonance R0 decreases in frequency with increasing glottal aperture. The mechano-acoustic impedance maximum $\bar{\text{R}}$0, which was evident with the glottis closed, no longer appears as a separate maximum, but acts to increase the frequency of the first impedance maximum of the combined ducts $\bar{\Sigma}$1.

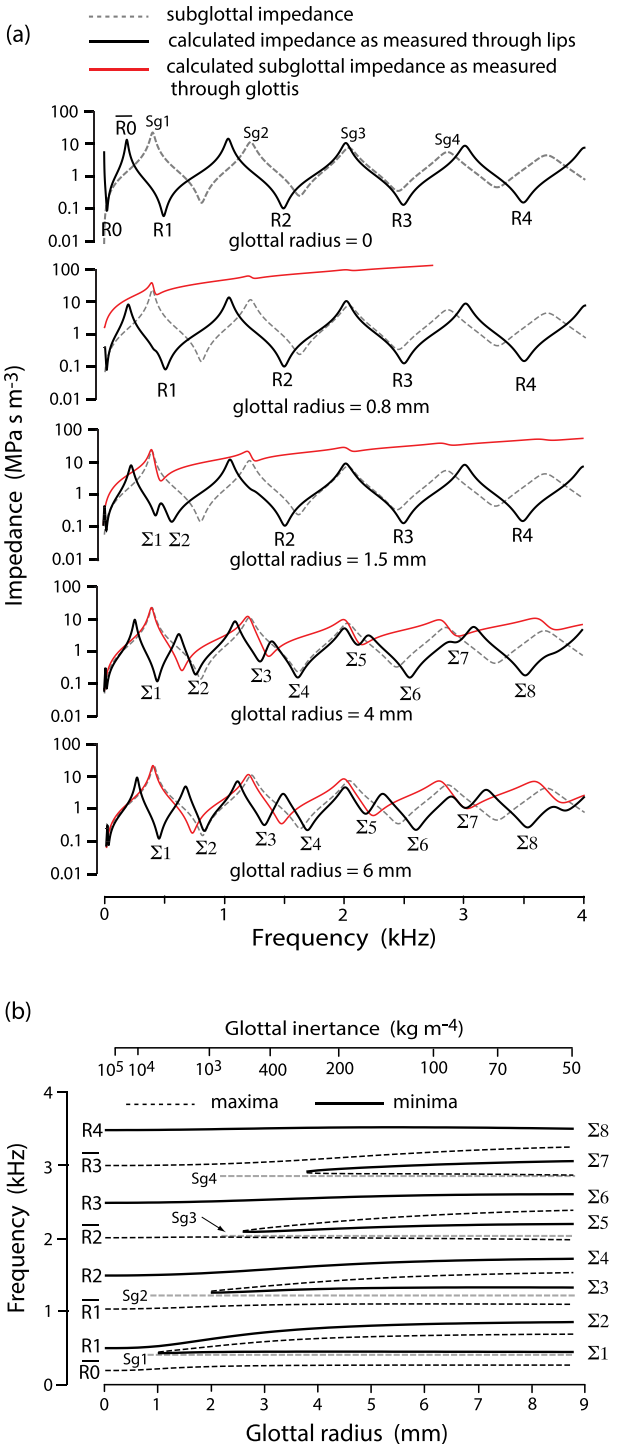

FIG. 3. (Color online) The effect of glottal inertance, shown also in terms of glottal radius, on the calculated impedance magnitude through the lips Z_{lip}. (a) Shows how the impedance through the lips (black line) varies with frequency for five different glottal radii; the impedance of the subglottal tract (dashed line) and its impedance seen through the glottis (red or gray line) are also shown. (b) Shows how the maxima (black dashed line) and minima (black continuous line) in Z_{lip} vary with the glottal inertance or radius. The values of the maxima in the subglottal impedance are indicated by the gray horizontal dashed lines. Parameters were $l_{\text{Vt}} = 170$ mm, $r_{\text{Vt}} = 11$ mm, $l_{\text{g}} = 10$ mm, $r_{\text{Sg}} = 9.5$ mm, $l_{\text{Sg}} = 200$ mm.

Figure 3 is calculated using a subglottal tract with effective length longer than that of the supraglottal tract; consequently in Fig. 3(a) the maxima in the subglottal impedance Sgi (pale dashed curve) occur at lower frequencies than the

corresponding minima in the input impedance of the supraglottal tract alone (black curve)—compare f_{Sgi} with f_{Ri}. As the glottal radius increases, and so the glottal inertance decreases, the maxima of the subglottal impedance will increasingly become apparent in the impedance seen through the glottis. This change in the acoustic load acting on the supraglottal tract will affect the impedance measured through the lips. Once the impedance through the glottis becomes comparable in magnitude with the supraglottal impedance, slight perturbations in the impedance measured through the lips will become evident around the value of subglottal impedance peaks f_{Sgi}; for example, see the curve for $r_g = 0.8$ or 1.5 mm in Fig. 3(a). As the glottal inertance decreases, the subglottal maxima f_{Sgi} will become increasingly apparent in the impedance seen through the glottis (red or gray line); this in turn will alter the local slope of the impedance seen through the lips until eventually a new pair of extrema will develop around each f_{Sgi}, for example, see $r_g = 4$ and 6 mm in Fig. 3(a).

Figure 3(b) shows this in more detail. Because the first maximum in the subglottal impedance is lower than R1, the new pair of extrema will occur at a frequency below R1. The frequency of the new minimum ($\Sigma 1$) will hardly change as r_g increases. R1 will increase in frequency as it becomes $\Sigma 2$. However, in this case the maximum $\bar{R}1$ remains substantially unchanged.

Whether the subglottal or supraglottal tract has a greater effective length could depend on which vowel is articulated. If the effective length of the subglottal tract is shorter than that of the supraglottal tract, the relationships between R1 and $\Sigma 1$ are different—see Fig. 4. In this case, the frequency of R1 will remain almost constant as it becomes $\Sigma 1$, while the new minimum that is introduced at a higher frequency becomes $\Sigma 2$. Similar observations apply to the extrema at higher frequencies. Now that the airway model is asymmetric with cylindrical sections of different length, the maxima no longer approach equal spacing at large glottal radius.

Figures 3 and 4 show that the frequencies at which each pair of new extrema first occur in Z_{lip} are often slightly above the frequency of the relevant maximum Sgi in the subglottal impedance $Z_{Sg} = R_{Sg} + jX_{Sg}$, as indicated by pale dashed lines in Figs. 3–5. This difference can be quite small, particularly for high values of the glottal inertance L_g. The maxima in Z_{Sg} will occur when $X_{Sg} = 0$. However, the new extrema in Z_{lip} actually form at a frequency determined by the subglottal impedance in series with the impedance of the glottis, i.e., the red curves in Fig. 3(a). These minima will occur when $Z_{Sg} + j\omega L_g = 0$, i.e., when $\omega L_g = -X_{Sg}$. Consequently, the frequencies at which new extrema occur will always be greater than the relevant f_{Sgi}.

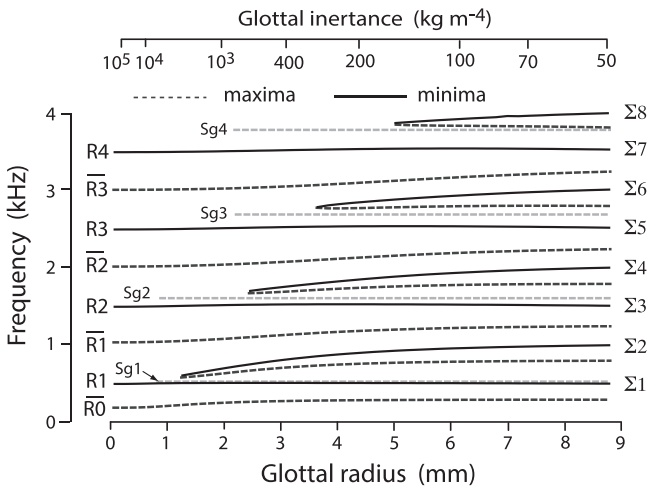

FIG. 4. As for Fig. 3 except with a shorter subglottal tract ($l_{Vt} = 17$ cm, $l_{Sg} = 15$ cm).

D. A model based on MRI

To investigate a more realistic model, calculations are made using a two-dimensional (mid-sagittal) airway profile measured from Magnetic Resonance Imaging (MRI) in a previous study that involved subject 7 (Appendix A, Table I, Hanna *et al.*, 2016b).

Figure 1(b) shows the airway radius (assuming cylindrical geometry) measured at 2 mm intervals along a smoothed centroid between the airway walls. The MRI from which these data were measured was made during phonation with subject 7 of the current study performing the same tasks as in Sec. III C with a plastic pipe of the same dimensions replacing the impedance head between his lips. As such the airway profile begins at the lips and includes the supraglottal tract, (open) glottis, and part of the subglottal tract with a length $l_{MRI} = 92$ mm in which no branching occurs. The remaining subglottal region associated with the bronchi and the lungs is replaced with an open

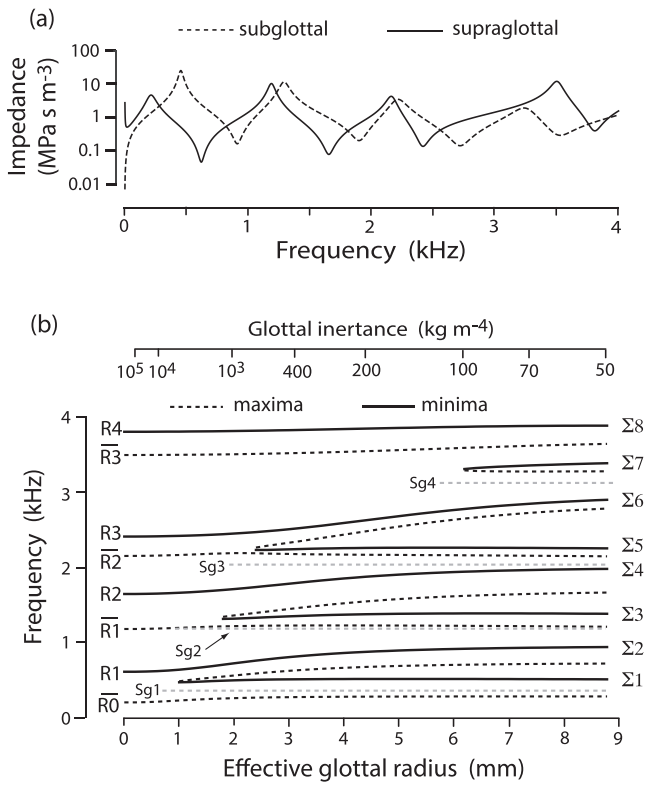

FIG. 5. The calculated impedance through the lips for a model with geometry based upon MRI for subject 7 during phonation (Hanna *et al.*, 2016b). The upper figure (a) compares the impedance magnitude of the supraglottal tract measured with closed glottis to that of the subglottal tract. The lower figure (b) shows the effect of decreasing glottal inertance, or increasing effective glottal radius, on the frequencies of the maxima and minima in the impedance measured through the lips.

TABLE I. Mean ± standard deviation of impedance measurements on seven male subjects during inspiration.

Impedance Minimum	Σ1	Σ2	Σ3	Σ4	Σ5	Σ6	Σ7
Frequency (Hz)	530 ± 60	880 ± 55	1335 ± 145	1735 ± 70	2210 ± 75	2565 ± 95	3660 ± 270
Effective length l_Σ (m)	0.32 ± 0.04	0.39 ± 0.02	0.38 ± 0.04	0.39 ± 0.02	0.38 ± 0.01	0.40 ± 0.01	0.33 ± 0.02
No. samples	281	261	252	159	127	209	173
Impedance Maximum	$\bar{\Sigma}1$	$\bar{\Sigma}2$	$\bar{\Sigma}3$	$\bar{\Sigma}4$	$\bar{\Sigma}5$	$\bar{\Sigma}6$	$\bar{\Sigma}7$
Frequency (Hz)	240 ± 50	725 ± 70	1090 ± 85	1530 ± 65	1930 ± 95	2315 ± 75	3080 ± 185
Effective length l_Σ (m)	0.35 ± 0.08	0.35 ± 0.03	0.39 ± 0.03	0.39 ± 0.02	0.40 ± 0.02	0.40 ± 0.01	0.36 ± 0.02
No. samples	319	263	243	201	162	147	181

cylinder of adjustable length l^*_{Sg} with a radius that matches the radius of the final MRI segment. The total subglottal length $l_{Sg} = l^*_{Sg} + l_{MRI}$. Partly because the image is limited, but mainly because the trachea is not actually terminated by a flange whose position could be measured, the missing length l^*_{Sg} was found by subsequent curve fitting—see Sec. IV B.

The calculated subglottal impedance (upstream of the glottis) and supraglottal impedance (through the lips with the glottis closed) are shown in Fig. 5(a). The extrema in both curves are now no longer evenly spaced. The maxima in the subglottal impedance occur at frequencies below the relevant minima in the supraglottal impedance. Consequently, the first pair of new extrema will occur at a frequency below f_{R1}. The wide spacing between extrema in subglottal and supraglottal impedance (with glottis closed) at higher frequencies mean that the full set of extrema might not be observed until the glottis is opened fairly wide.

E. Deriving parameter values from experimental data

Figures 3, 4, and 5 show that information on the subglottal impedance could be determined if measurements were available as a function of r_g. However, the simplest measurements made on subjects will usually have Z_{lip} measured for only two values of r_g; one with the glottis closed, corresponding to $r_g = 0$, and another during respiration with an unknown, but probably large value of r_g. If a pair of adjacent minima with very small relative magnitudes is apparent, then the relevant maximum in the subglottal impedance will be slightly below this value. However, this would depend upon the subject using a suitable value of r_g, and at best could only work for one maximum in each measurement.

If measurements are made with a relatively open glottis such that the additional extrema are clearly apparent, the subglottal lengths can be calculated assuming a cylindrical model.

III. MATERIALS AND METHODS

A. Impedance spectrometry through the lips

Impedance spectrometry was performed with the three-microphone-three-calibration technique (Dickens *et al.*, 2007) in the configuration shown in Fig. 6, as previously described (Hanna *et al.*, 2016a). Briefly, a broadband signal is synthesised as a sum of sine waves with amplitudes and phases chosen to improve the signal-to-noise ratio (Smith, 1995). For studying steady conditions (either closed glottis, inspiration, or expiration), the usual frequency range was 14 to 4200 Hz with a spacing of 2.69 Hz. However, for three subjects this frequency range resulted in an inadequate signal-to-noise ratio and the range was reduced to 200 to 4200 Hz, so that more audio power could be concentrated in the reduced range. For the measurements of transient behaviour (transitions from inspiration to expiration), the frequency resolution was decreased to 10.8 Hz. The impedance head and microphones are calibrated with three non-resonant loads: an acoustically infinite waveguide, a large mass (quasi-infinite impedance), and the radiation impedance with a large baffle. From the three microphone signals, the traveling waves in both directions are deduced, and from these the impedance at the measurement plane is calculated as a function of frequency. The impedance extrema are then identified from the spectra and fitted with parabolas to determine their frequency f, impedance magnitude $|Z|$, and bandwidth B, as described in Hanna *et al.* (2016a).

B. Subjects

Ten volunteer subjects (seven men and three women) participated in the study, the same subjects as described in Table I of Hanna *et al.* (2016a). All subjects were non-smokers and none reported a history of voice disorders. The experiments were conducted in a room treated to reduce reverberation and external noise. The design of the study was approved by the university's human ethics committee.

C. Experimental protocol

The subjects were instructed to find a comfortable position for the impedance head in the mouth and to ensure an airtight seal with their lips around the outer diameter of 31.8 mm. The subjects were asked to keep their tongue in the position to pronounce the word "heard" (approximately the neutral vowel /ɜ/ in Australian English—Delbridge, 1981) with their velum closed to avoid nasalisation for the duration of the injected broadband signal.

Most measurements consisted of the injection of 10 or 18 contiguous cycles of the broadband signal, lasting 3.7 or 6.7 s, through the measurement head between the lips and into the subject's respiratory airway. At least three measurements were made for each subject: (a) breathing in (inspiration), (b) breathing out (expiration) at a relaxed rate, and (c) miming with a closed glottis. Preliminary experiments showed that a very rapid inspiration produced measured impedance spectra that differed most from those with the closed glottis condition. However, as rapid inspiration can easily achieve full lung capacity in less than the duration of the measurement, subjects were given time to practice matching their inspiration length to the duration of the probe signal. The first and last cycles of

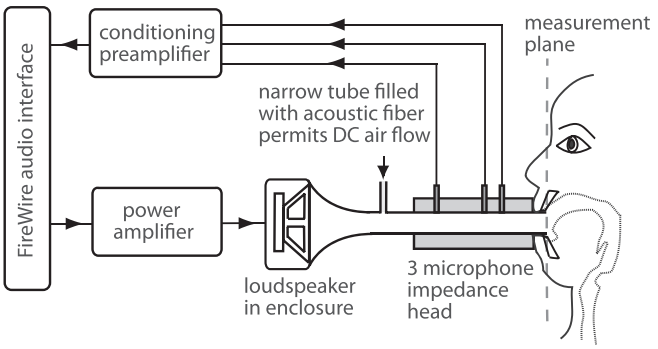

FIG. 6. Schematic diagram (not to scale) showing how the airway impedance was measured through the lips.

the signals recorded by the three microphones were discarded to exclude any possible transients.

IV. RESULTS AND DISCUSSION

A. Impedance measurements during respiration

1. Transition from expiration to inspiration

Figure 7 shows a sequence of impedance spectra measured during the transition from expiration to closed glottis to inspiration by subject 7 (male). The spectra of eight (non-consecutive) frames, each of 93 ms duration, are shown from a sequence of 50 frames lasting 4.6 s for the whole cycle of respiration. Their global features are described using the simple model and the nomenclature developed in Sec. II.

The top spectrum [Fig. 7(a)] shows the midpoint of expiration. The minima are $\Sigma 1-4$, R3, and R4. The second and third spectra show the cycles immediately preceding glottal closure. In Fig. 7(b), $\Sigma 1$ and $\Sigma 2$ are still present, but the glottal inertance has increased sufficiently to replace $\Sigma 3$ and $\Sigma 4$ with a slightly perturbed R2. In Fig. 7(c), R1 is also reintroduced, although again with slight perturbation. The spectrum in Fig. 7(d) is representative of the closed glottis portion of the respiration cycle with purely supraglottal resonances $R1-4$ appearing as expected. Spectra [Figs. 7(e)–7(g)] show the opening of the glottis to begin inspiration. Initially R1 and R2 are replaced by $\Sigma 1-4$, followed by $\Sigma 5$ and $\Sigma 6$ replacing R3. Figure 7(h) shows the midpoint of inspiration, in which the six minima $\Sigma 1-6$ are approximately regularly spaced. The curves are qualitatively similar to those in Fig. 3.

The rapid 93 ms measurements in this series have a frequency resolution of only 10.8 Hz ($=44\,100/2^{12}$), compared with the frequency resolution of 2.69 Hz ($=44\,100/2^{14}$) used for the longer, 0.37 s cycle measurements reported below. They also have an inferior signal-to-noise ratio. Nonetheless, the frequency resolution and signal-to-noise ratio are sufficient to observe changes in impedance spectra and to demonstrate that this technique can be used to make rapid measurements during normal respiration.

2. Inspiration

Figure 8 shows representative impedance spectra for the closed glottis and inspiration conditions measured over one 0.37 s frame for each of the subjects. The low frequency

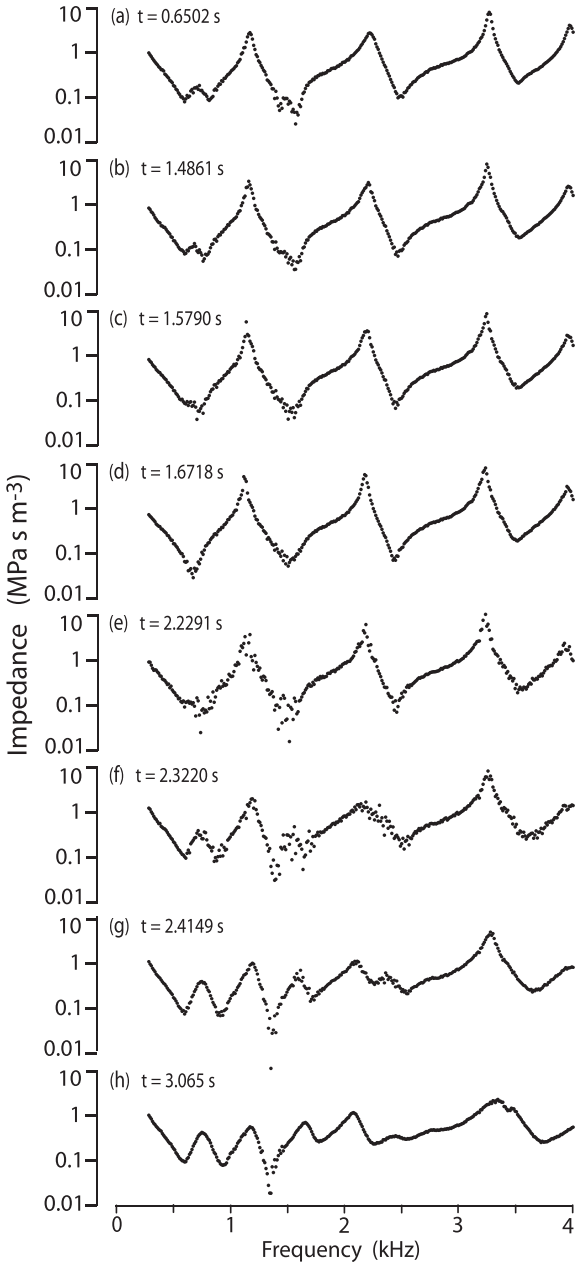

FIG. 7. Impedance magnitude spectra measured through the lips at different times during a single transition from expiration to closed glottis to inspiration. A video showing a looped version of the full sequence of 50 measurements is included in the supplemental material.[2]

(below 300 Hz) features are due to the non-rigidity of the duct: the maximum at approximately 200 Hz ($\bar{R}0$) is due to the mass of tissue surrounding the duct oscillating on the "spring" of the air sealed inside; the minimum around 20 Hz (R0) is caused by the same mass supported on the spring of its own tissue elasticity. (On the scale used here, R0 is difficult to see but is evident on the closed glottis data for subjects 2, 4, and 5. For a more detailed study of R0, see Hanna *et al.*, 2016a.)

For the inspiration data, the effective length of the duct is approximately doubled and the remote end of the duct, as suggested by the simple model of Lulich *et al.* (2011), is effectively that of an open tube—see Figs. 2(e) and 3. Hence some of the inspiration curves in Fig. 8 have twice as many

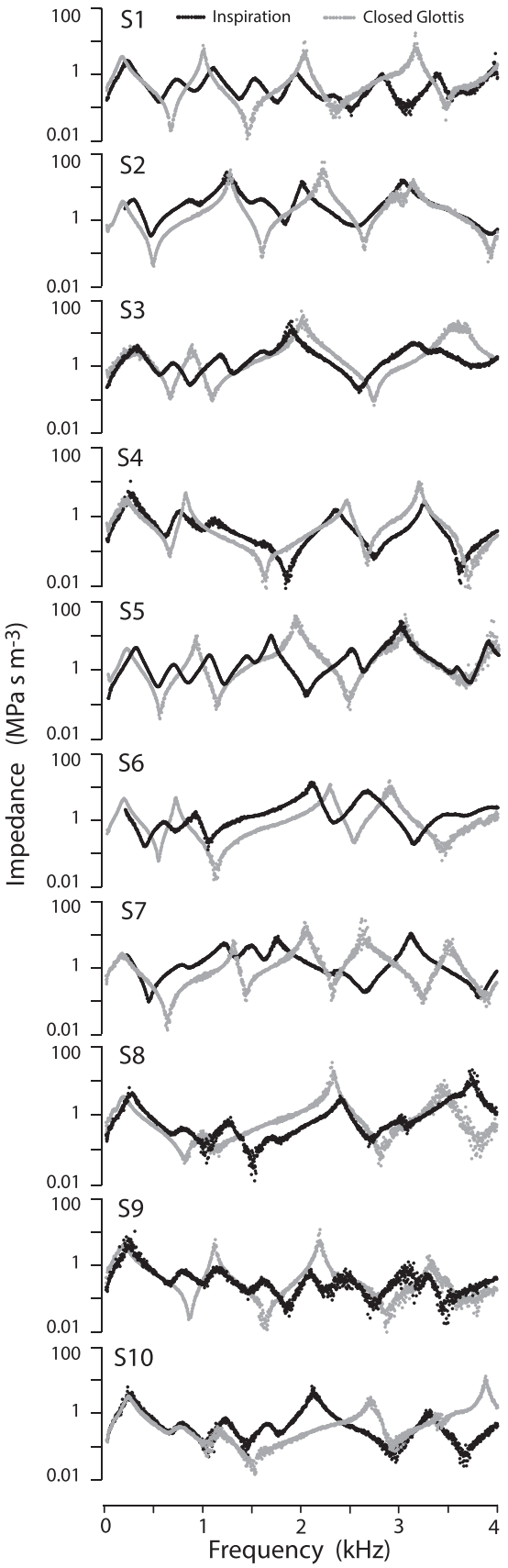

FIG. 8. Typical impedance magnitude spectra Z_{lip} measured during a single cycle (370 ms) for closed glottis (pale line) and during inspiration (dark line) over the range 14–4200 Hz. Note, the inspiration data for subjects 2, 6, and 7 were measured over a reduced range (200–4200 Hz) due to an insufficient signal-to-noise ratio over the wider frequency range.

extrema as the closed glottis curves; in others only the Σi and $\bar{\Sigma}$i at lower frequencies are seen, presumably because the glottis is less open and its higher inertance seals the tract at high frequency, as shown in Figs. 2 and 3. The frequencies of the minima Σi and maxima $\bar{\Sigma}$i are given in Tables I and II. The data for individual subjects are given in Table IV.

For any one subject, the standard deviation in the measured frequency of the impedance minima $f_{\Sigma i}$ and maxima $f_{\bar{\Sigma}i}$ was low for the combined tract. For some subjects, the glottal inertance appeared to be too high to affect the higher frequencies, hence there are fewer data for $\Sigma 5-7$.

The variability between subjects shown in Tables I and II for each of the $f_{\Sigma i}$ and $f_{\bar{\Sigma}i}$ was modest (an average standard deviation of 8% for men and 6% for women).

The effective length l_Σ of the combined tract shown in Tables I and II was calculated using $l_{\bar{\Sigma}i} = (2i - 1)c/(4\, f_{\bar{\Sigma}i})$ for maxima and $l_{\Sigma i} = ic/(2\, f_{\Sigma i})$ for minima; this assumes that each resonant frequency is due to a standing wave in an open duct and relaxes the requirement that the tract is cylindrical by treating each resonance separately. For any given extremum, the effective length of the combined tract is quite similar, at about 37 ± 4 cm for men and 34 ± 3 cm for women. This gives some *post hoc* justification for the simple geometrical models used above. The first resonance $\Sigma 1$ of the combined duct gives a considerably shorter effective length than the subsequent resonances (if $f_{\Sigma 1}$, $f_{\bar{\Sigma}1}$, $f_{\Sigma 7}$, and $f_{\bar{\Sigma}7}$ are excluded then $l_\Sigma = 39 \pm 3$ cm for men and 35 ± 2 cm for women). Frequency ratios in which the first member is greater than that in a 1:3:5 ratio have been previously noted for the first subglottal resonance by other researchers and attributed, at least in part, to tracheal wall properties.

3. Expiration

Measurements made during gentle expiration (Wolfe *et al.*, 2013) show little qualitative difference from phonation measurements (Hanna, 2014), except that the former lack a harmonic voice signal at f_o, $2f_o$, etc. This suggests that the glottal inertance associated with a small effective glottal aperture largely decouples the two ducts at all but very low frequencies (below R1), and that the inertance of the glottis is considerably larger for gentle expiration than for inspiration. However, the glottal aperture during expiration is variable, so at times there can be measurable coupling to the subglottal tract (see Fig. 7) to an extent comparable with inspiration. Due to this variability, the expiration measurements are not discussed in detail. Figure 9 shows one example of subject 7 during a deep and rapid respiration cycle in which $\Sigma 1-6$ are visible in both the inspiration and expiration data, cf. the more natural respiration cycle in Fig. 7 in which only $\Sigma 1-4$ are visible during expiration, suggesting a smaller glottal aperture.

Figure 9 shows that $f_{\Sigma i}$ and $f_{\bar{\Sigma}i}$ in the expiration measurements either occur at a frequency similar to or lower than in the inspiration measurements; this suggests a higher glottal inertance during expiration (e.g., see Figs. 3–5). Developments of the present technique could be useful for monitoring irregularities in respiration, such as changes in airway geometry, or even airway compliance, data which are perhaps useful for obstructive sleep apnea.

TABLE II. Mean ± standard deviation of impedance measurements on three female subjects during inspiration.

Impedance Minimum	$\Sigma 1$	$\Sigma 2$	$\Sigma 3$	$\Sigma 4$	$\Sigma 5$	$\Sigma 6$	$\Sigma 7$
Frequency (Hz)	660 ± 30	1020 ± 45	1490 ± 45	1820 ± 65	2460 ± 55	2790 ± 160	3680 ± 455
Effective length l_Σ (m)	0.26 ± 0.01	0.33 ± 0.02	0.34 ± 0.01	0.37 ± 0.01	0.35 ± 0.01	0.37 ± 0.01	0.32 ± 0.02
No. samples	103	32	14	63	34	67	33
Impedance Maximum	$\bar{\Sigma}1$	$\bar{\Sigma}2$	$\bar{\Sigma}3$	$\bar{\Sigma}4$	$\bar{\Sigma}5$	$\bar{\Sigma}6$	$\bar{\Sigma}7$
Frequency (Hz)	260 ± 35	785 ± 60	1200 ± 60	1680 ± 70	2170 ± 60	2505 ± 180	3480 ± 205
Effective length l_Σ (m)	0.33 ± 0.04	0.32 ± 0.02	0.35 ± 0.02	0.35 ± 0.01	0.35 ± 0.01	0.37 ± 0.03	0.32 ± 0.02
No. samples	182	117	103	104	67	112	81

B. Estimating subglottal parameters from impedance spectra through the lips

1. Fitting to a model based on MRI measurements

In a model that better approximates the actual airway geometry, the cylindrical supraglottal cylindrical tube is replaced with a series of cylinders of length 2 mm with radius derived from MRI measurements of subject 7 during phonation (Hanna *et al.*, 2016b). The radius as a function of distance from the lips is shown in Fig. 1(b) and discussed in Sec. II D. The supraglottal tract and glottis are specified by the MRI radius and length. The initial part of the subglottal tract of length l_{MRI} is also based upon the MRI data, but the final part of length l^*_{Sg} is treated as a flanged, uniform cylinder. This length l^*_{Sg} is now a free parameter in an otherwise geometrically specified model.

Figure 10(a) shows three closed glottis acoustic impedance measurements, i.e., supraglottal tract only, made in supine position to match the MRI procedure, each measured over 12 contiguous cycles (each 370 ms) resulting in a total of 36 pale curves. Note that $f_{\mathrm{R}1}$, $f_{\mathrm{R}2}$, and $f_{\mathrm{R}3}$ occur at higher frequencies in one of the three impedance measurement sets. These are compared with the impedance calculated using the radius as a function of length derived from the MRI, but with a rigid termination at the glottis and using the wall loss and mechanical parameters described previously. The acoustic data measured with a closed glottis show reasonable agreement with the calculated impedance: the difference between model and measurement is of the same order as that between different measurements on the same subject under (nominally) the same conditions. For example, note the grouping into two distinct positions of the maxima $\bar{\mathrm{R}}3$ in the gray curves.

To model the case of inspiration, the glottal and subglottal radii from MRI are used and the missing length l^*_{Sg} to the duct termination by a large flange is adjusted manually to a best fit, giving a total effective $l_{\mathrm{Sg}} = 177$ mm. The results of this fit are shown in Fig. 10(b).

The aim of the modeling in this study is to illustrate the effects of the subglottal tract on the impedance measured through the lips rather than to provide accurate anatomical detail. Further improvements could be made by adjusting more parameters to provide better agreement. However, it is encouraging to see that several of the features of Fig. 10(b) are reproducible with just one adjustable parameter: the length l^*_{Sg} to the acoustic subglottal termination (the glottal radius r_{g} is made up of the five relevant cylindrical segments in the MRI data and not adjusted to fit).

2. Fitting to a simple cylindrical model

The MRI study of Hanna *et al.* (2016b) only involved subject 7 (male). For all other subjects, a simpler geometric model was fitted, treating each of the tracts and the glottis as a separate cylinder, with deformable, lossy walls. The fitting was performed first on the closed glottis data by adjusting the length of the supraglottal tract l_{Vt}, then the parameters that describe the series mechanical resonance, i.e., the tissue inertance L_{t}, compliance C_{t}, and loss term b_{R}. In the absence of specific information, the mean r_{Vt} from the MRI data was used for all subjects. Next, assuming the same mechanical parameters, the subglottal tract length l_{Sg} and the glottal radius r_{g} were fitted to the inspiration data—see Table III. The subglottal tract estimated in this fashion has an effective length range of $l_{\mathrm{Sg}} = 170$–220 and 170–190 mm for the men and women in this study, respectively. [Lulich *et al.* (2011) reported a range of 180–235 mm including both sexes for the same simple, flanged, uniform duct model.]

TABLE III. The fitted parameters for each subject found by fitting to the simple cylindrical model. L_{t} and C_{t} are the distributed tissue inertance and compliance of the supraglottal vocal tract, and b_{R} is the resistive loss.

Subject	1	2	3	4	5	6	7	8	9	10
Fitted parameters for closed glottis measurements										
l_{VT} (mm)	185	180	180	165	170	165	175	160	160	165
L_{t} (kg m^{-4})	2000	1000	1400	1200	500	2000	1200	2000	1000	600
C_{t} (m^3 Pa^{-1})	5×10^{-8}	3×10^{-8}	3×10^{-8}	5×10^{-8}	10×10^{-8}	3×10^{-8}	6×10^{-8}	3×10^{-8}	8×10^{-8}	10×10^{-8}
b_{R} (Pa s m^{-3})	4×10^{5}	2×10^{5}	5×10^{5}	3×10^{5}	3×10^{5}	7×10^{5}	5×10^{5}	4×10^{5}	3×10^{5}	2×10^{5}
Fitted parameters for inspiration measurements										
Model l_{Sg} (mm)	180	220	200	170	180	180	210	170	190	175
Model r_{g} (mm)	4	3	4	3	4	3	5	3	4	4

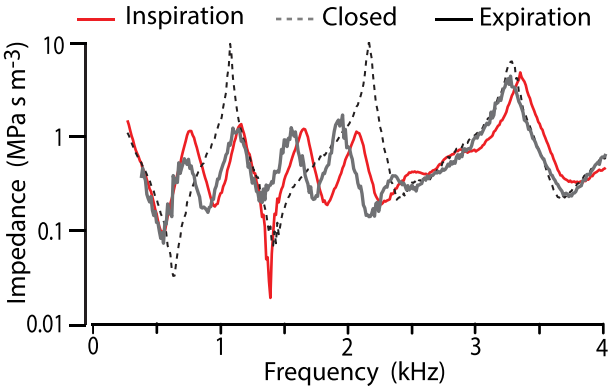

FIG. 9. (Color online) The impedance magnitude measured with a closed glottis (pale dashed line), during inspiration (red or gray line), and during expiration (black line) during a single cycle of deep and rapid respiration.

3. Estimation from resonance frequencies

Another estimate of subglottal length can be made by taking the total length of both tracts using the $f_{\Sigma i}$ values in Table IV and calculating, then subtracting the modelled lengths of the supraglottal tract, obtained from the closed glottis measurements, and the length of the glottis. Recall that different subjects showed different numbers of Σi, presumably due to differences in their glottal aperture for inspiration. Table IV shows only $f_{\Sigma 1-3}$, since these were observed in all subjects. However, all available $f_{\Sigma i}$ for each subject were used to give the calculated lengths, which give a range of $l_\Sigma = 340$–420 mm and $l_{Sg} = 175$–210 mm for men, and $l_\Sigma = 320$–330 mm and $l_{Sg} = 160$–165 mm for women.

The last two rows of Table IV give the height of the subjects and the expected subglottal length calculated using the expression of height divided by a gender appropriate empirical scaling factor from Lulich *et al.* (2011). The subglottal length calculated in this way is expected to be longer (as observed) for two reasons. First, the calculation assumes a speed of sound of 359 m/s rather than the 340 m/s used for calculations in this paper (a difference in length of ~6%). Second, the calculation assumes that f_{Sg2} and f_{Sg3} are more accurate predictors of l_{Sg} than f_{Sg1}. As a simplification, assuming that $f_{\Sigma 1} = f_{Sg1}$ and $f_{\Sigma 3} = f_{Sg2}$ as implied by Figs. 3 and 4, then f_{Sg1} would indeed be on average higher than expected for a simple uniform tube model ($f_{Sg1}:f_{Sg2} = 1{:}2.5$ rather than 1:3). Excluding the measured $f_{\Sigma 1}$ from the calculation increases the effective length and therefore also the subglottal length by 1 cm for both men and women.

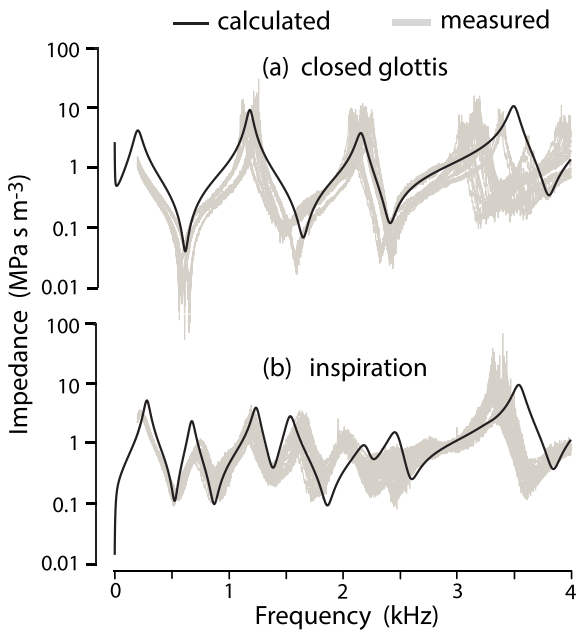

FIG. 10. (Color online) Acoustic impedance measurements through the lips (pale lines) and the calculated acoustic impedance (dark line) using an MRI airway profile of the same subject with only the length l^*_{Sg} as the single free parameter. The impedance measurements show the superposed results of 12 frames in each of three separate measurements (a total of 36 curves).

In principle, one could correct for the high f_{Sg1} by involving a flexible *conus elasticus* or a trachea and cartilage model (Lulich and Arsikere, 2015). However, the range of differences between $f_{\Sigma 1}$ and f_{Sg1} makes such modeling unreliable.

Lulich *et al.* (2011) made measurements of the vibration of the skin of the neck below the glottis. They reported ranges for the vibrational maxima: 400–900, 1100–1700, and 1800–2600 Hz for 25 male and 25 female subjects. In each case, the range of values reported is sufficiently broad that the values of both $f_{\Sigma i}$ and $f_{\overline{\Sigma} i}$ for i = 1, 2, 3, in Table IV of the present study fall within them. However, to determine the frequencies of the subglottal resonances f_{Sgi} and anti-resonances $f_{\overline{Sgi}}$ from accelerometer measurements requires assumptions about the glottal source, its opening area, the extent to which the supraglottal tract appears in parallel, and the relevant transfer functions. To determine these frequencies from the measurements in the present study similarly requires approximations and modeling.

TABLE IV. Measured frequencies and calculated lengths.

Subject	1	2	3	4	5	6	7	8	9	10
$f_{\overline{\Sigma}1}$ (Hz)	220 ± 10	170 ± 80	270 ± 15	255 ± 30	320 ± 15	265 ± 20	210 ± 20	255 ± 25	280 ± 45	245 ± 25
$f_{\Sigma 1}$ (Hz)	495 ± 40	495 ± 25	535 ± 20	620 ± 20	505 ± 25	450 ± 15	550 ± 15	675 ± 25	670 ± 25	640 ± 25
$f_{\overline{\Sigma}2}$ (Hz)	775 ± 25	680 ± 20	610 ± 40	775 ± 30	705 ± 20	870 ± 25	720 ± 20	785 ± 35	850 ± 50	740 ± 35
$f_{\Sigma 2}$ (Hz)	875 ± 30	830 ± 35	835 ± 30	945 ± 60	820 ± 20	910 ± 35	915 ± 20	1035 ± 15	980 ± 30	1055 ± 20
$f_{\overline{\Sigma}3}$ (Hz)	1165 ± 60	1005 ± 25	1005 ± 25	1065 ± 90	1225 ± 25	1280 ± 10	1100 ± 30	1255 ± 55	1170 ± 40	1175 ± 45
$f_{\Sigma 3}$ (Hz)	1335 ± 25	1115 ± 40	1120 ± 25	1575 ± 30	1320 ± 35	1480 ± 15	1375 ± 20	1485 ± 60	1465 ± 10	1525 ± 50
Calculated l_Σ (mm)	370	420	390	340	350	350	370	320	320	330
Calculated l_{Sg} (mm)	185	240	210	175	180	185	195	160	160	165
Height (m)	1.83	1.84	1.78	1.71	1.65	1.78	1.84	1.70	1.77	1.74
Scaled l_{Sg} (mm) from height	215	216	209	201	194	210	216	200	208	205

C. Implications of subglottal resonances for the spectral envelope of the voice

It has been argued that extrema in the acoustic impedance of the subglottal tract, "seen" at the glottis, Z_{Sg}, might affect the output sound. Extra formants and antiformants may appear, for example in aspirated sounds (Fant *et al.*, 1972; Stevens, 2000), and formants may undergo changes in bandwidth and frequency (Fujimura and Lindqvist, 1971).

Other effects might be due to the acoustic pressure at the glottis affecting the motion of the vocal folds. In models of auto-oscillating valves in which the motion is primarily longitudinal, the acoustic pressure difference acting on the valve is approximately the series impedance of the two ducts, supra- and subglottal (Benade, 1985). In Fletcher's models of auto-oscillation (1993), this is called the "outward swinging door" model. There is also a model in which the two ducts appear in parallel as an acoustic load: if the volume of the glottis varies independently of the volume of the upstream and downstream tracts, and if some portion of the glottis remains open throughout the cycle (Fletcher's "sliding door" model). For the purposes of such considerations, Fig. 11 shows the calculated impedance seen by the glottis due to the series and parallel impedance combinations of the sub- and supraglottal tracts using the MRI based airway profile with adjusted l^*_{Sg}, and assuming that the supraglottal tract was terminated with a plane baffle at the lips. One difference between the series and parallel loads on the glottis is that the series load displays additional resonances. (Neither series nor parallel combination has a simple relation to the measurements made in this study.)

It might be anticipated that auto-oscillation would be disturbed in frequency ranges over which the magnitude or sign of the acoustic load on the glottis varied rapidly as a function of frequency (Zhang *et al.*, 2006; Titze 2008). The soprano voice can cross the frequencies of the first sub- and supraglottal resonances. However, experiments on female singers performing pitch glides in the ranges of both sub- and supraglottal resonances showed no clear clustering of instabilities around the subglottal resonance frequencies (Titze *et al.*, 2008; Wade *et al.*, 2017).

D. Implications for voice synthesis

Voice synthesis using typical modal (M1) phonation does not use information about the subglottal tract. In this case, a simple model of source and independent supraglottal vocal tract as a filter may yield satisfactory results. Producing realistic synthesised breathy voices or breathing sounds, however, might benefit from inclusion of the resonant properties of the subglottal tract.

E. Implications for estimating tracheal and glottal geometry

Can impedance spectrum measurements through the lips give information about constrictions in the trachea or bronchi? At the frequencies considered here, only the trachea and the first few branches contribute: the rest are included in the flange used to model the rapidly increasing cross section. At the current stage, diagnostics of constrictions in these areas are, sadly, beyond current modeling. Nevertheless, the current understanding and measurement technology are sufficient for monitoring changes in the acoustic impedance during respiration, as shown in Fig. 9.

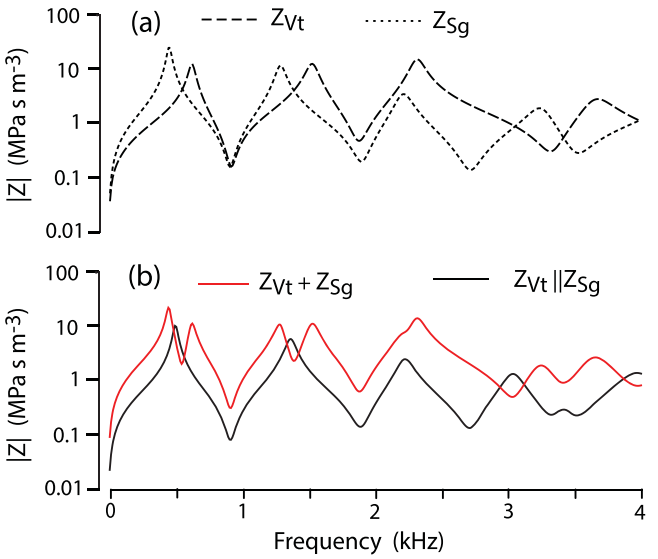

FIG. 11. (Color online) The top graph (a) shows the magnitude of the sub- and supraglottal impedances (Z_{Sg} and Z_{Vt}, respectively) as seen by the glottis and calculated from the MRI based airway profile and the fitted final part of the subglottal length l^*_{Sg}. (b) shows the calculated magnitude of the load impedances for their series ($Z_{Vt} + Z_{Sg}$) and parallel $Z_{Vt} \| Z_{Sg}$ [$=Z_{Vt} \cdot Z_{Sg}/(Z_{Vt} + Z_{Sg})$] combinations.

V. CONCLUSIONS

When the glottis is closed, the impedance spectrum measured through the lips for the neutral vowel /ɜ/ reveals minima Ri and maxima $\bar{\text{R}}$i similar to those expected for a closed cylindrical duct. When the glottis is gradually opened, as occurs during respiration, the inertance of the glottis that connects the sub- and supraglottal tracts is gradually reduced. Maxima in the subglottal impedance Sgi then increasingly affect the measured impedance producing additional pairs of maxima $\bar{\Sigma}$i and minima Σi. Because the glottal inertance increases with frequency, these additional extrema are first evident at low frequencies. With the glottis open for inspiration, and the mouth closed around an impedance head, the combined supra- and subglottal tracts behave rather similarly to an open duct of effective length $l_\Sigma = 37 \pm 4$ for men and 34 ± 3 cm for women. The average length of the subglottal tract in isolation calculated from the measured resonance frequencies using $l_{Sg} = l_\Sigma - l_{Vt}$ was 19.5 cm for the men and 16.0 cm for the women in this study. Excluding $f_{\Sigma 1}$ and $f_{\bar{\Sigma} 1}$ from the calculation, since they are not close to the 1:3:5 frequency ratio of a uniform duct, increases the effective length l_Σ and therefore l_{Sg} by 1 cm for both men and women. Using visual curve fitting of the measured impedance spectra to a simple cylindrical model for each subject, l_{Sg} was 17–22 cm for men and 17–19 cm for women.

ACKNOWLEDGMENTS

This study was supported by the Australian Research Council. We thank our volunteer subjects for their

participation, and Jason Amatoury and Neville Fletcher for helpful discussions.

[1]Notation used in this paper follows Titze *et al.* (2015) and Hanna *et al.* (2016a) where the ith supraglottal vocal tract resonance Ri occurs at frequency f_{Ri}, with impedance Z_{Ri}. For a closed-open duct such as the supraglottal vocal tract, an acoustic resonance Ri ($i > 0$) occurs where a standing wave has a pressure maximum at the closed (glottis) end and a pressure minimum (atmospheric pressure) at the open (lip) end—a situation that would produce a formant, Fi, measured outside the mouth. Therefore, impedance maxima seen at the glottis are called resonances, Ri, and impedance minima are called anti-resonances, $\bar{R}i$. By analogy, if the subglottal tract is assumed to act as a duct effectively open at the lung end for acoustic frequencies, the impedance maxima, as seen from the glottis, are the subglottal resonances, Sgi, and the impedance minima are anti-resonances, $\overline{Sg}i$. The majority of discussion in this paper is based on measurements through the lips. From the lip end, the condition for a resonance Ri (a pressure minimum at the lips and maximum at the glottis) produces impedance minima, and the anti-resonances $\bar{R}i$ are therefore impedance maxima. Note also, R0 is a mechano-acoustic resonance and $\bar{R}0$ a mechano-acoustic anti-resonance as seen through the lips due to yielding wall properties.

[2]See supplementary material at https://doi.org/10.1121/1.5033330 for a video showing the full sequence of 50 successive measurements used to make Fig. 7, i.e., impedance spectra measured during a single transition from expiration to closed glottis to inspiration.

Benade, A. (**1985**). "Air column, reed, and player's windway interaction in musical instruments," in *Vocal Fold Physiology, Biomechanics, Acoustics, and Phonatory Control*, edited by I. R. Titze and R. C. Scherer (Denver Center for the Performing Arts, Denver, CO), Chap. 35, pp. 425–452.

Brown, N. J., Xuan, W., Salome, C. M., Berend, N., Hunter, M. L., Musk, A., James, A. L., and King, G. G. (**2010**). "Reference equations for respiratory system resistance and reactance in adults," Resp. Physiol. Neurobiol. **172**, 162–168.

Campbell, D., and Brown, J. (**1963**). "The electrical analogue of lung," British J. Anaesthesia **35**, 684–692.

Chi, X., and Sonderegger, M. (**2007**). "Subglottal coupling and its influence on vowel formants," J. Acoust. Soc. Am. **122**, 1735–1745.

Cranen, B., and Boves, L. (**1987**). "On subglottal formant analysis," J. Acoust. Soc. Am. **81**, 734–746.

Delbridge, A. (**1981**). *The Macquarie Dictionary* (Macquarie Library, St. Leonards, Australia), 820 pp.

Dickens, P., Smith, J., and Wolfe, J. (**2007**). "High precision measurements of acoustic impedance spectra using resonance-free calibration loads and controlled error distribution," J. Acoust. Soc. Am. **121**, 1471–1481.

Fant, G., Ishizaka, K., Lindqvist-Gauffin, J., and Sundberg, J. (**1972**). "Subglottal formants," STL-QPSR **13**(1), 1–12.

Fletcher, N. H. (**1993**). "Autonomous vibration of simple pressure-controlled valves in gas flows," J. Acoust. Soc. Am. **93**, 2172–2180.

Fredberg, J. J., and Hoenig, A. (**1978**). "Mechanical response of the lungs at high frequencies," J. Biomech. Eng. **100**, 57–66.

Fujimura, O., and Lindqvist, J. (**1971**). "Sweep-tone measurements of vocal-tract characteristics," J. Acoust. Soc. Am. **49**, 541–558.

Habib, R. H., Chalker, R. B., Suki, B., and Jackson, A. C. (**1994**). "Airway geometry and wall mechanical properties estimated from subglottal input impedance in humans," J. Appl. Physiol. **77**, 441–451.

Hanna, N. (**2014**). "Investigations of the acoustics of the vocal tract and vocal folds in vivo, ex vivo and in vitro," UNSW, Australia and Université de Grenoble, France, 120 pp.

Hanna, N., Amatoury, J., Smith, J., and Wolfe, J. (**2016b**). "How long is a vocal tract? Comparison of acoustic impedance spectrometry with magnetic resonance imaging," Proc. Meet. Acoust. **28**, 60001.

Hanna, N., Smith, J., and Wolfe, J. (**2012**). "Low frequency response of the vocal tract: Acoustic and mechanical resonances and their losses," in *Proceedings of the Australian Acoustical Society*, edited by T. McGinn, Fremantle, Australia, pp. 317–323.

Hanna, N., Smith, J., and Wolfe, J. (**2016a**). "Frequencies, bandwidths and magnitudes of vocal tract and surrounding tissue resonances, measured through the lips during phonation," J. Acoust. Soc. Am. **139**, 2924–2936.

Harper, P., Kraman, S. S., Pasterkamp, H., and Wodicka, G. R. (**2001**). "An acoustic model of the respiratory tract," IEEE Trans. Biomed. Eng. **48**, 543–550.

Horsfield, K., Dart, G., Olson, D. E., Filley, G. F., and Cumming, G. (**1971**). "Models of the human bronchial tree," J. Appl. Physiol. **31**, 207–217.

Ishizaka, K., Matsudaira, M., and Kaneko, T. (**1976**). "Input acoustic-impedance measurement of the subglottal system," J. Acoust. Soc. Am. **60**, 190–197.

Lamarche, A., and Ternström, S. (**2008**). "An exploration of skin acceleration level as a measure of phonatory function in singing," J. Voice **22**, 10–22.

Lulich, S. M. (**2006**). "The role of lower airway resonances in defining vowel feature contrasts," Ph.D. thesis, Massachusetts Institute of Technology, pp. 32–46.

Lulich, S. M. (**2010**). "Subglottal resonances and distinctive features," J. Phonetics **38**, 20–31.

Lulich, S. M., Alwan, A., Arsikere, H., Morton, J. R., and Sommers, M. S. (**2011**). "Resonances and wave propagation velocity in the subglottal airways," J. Acoust. Soc. Am. **130**, 2108–2115.

Lulich, S. M., and Arsikere, H. (**2015**). "Tracheo-bronchial soft tissue and cartilage resonances in the subglottal acoustic input impedance," J. Acoust. Soc. Am. **137**, 3436–3446.

Lulich, S. M., Morton, J. R., Arsikere, H., Sommers, M. S., Leung, G. K., and Alwan, A. (**2012**). "Subglottal resonances of adult male and female native speakers of American English," J. Acoust. Soc. Am. **132**, 2592–2602.

Oostveen, E., MacLeod, D., Lorino, H., Farré, R., Hantos, Z., Desager, K., and Marchal, F. (**2003**). "The forced oscillation technique in clinical practice: Methodology, recommendations and future developments," Eur. Resp. J. **22**, 1026–1041.

Robinson, P. D., Turner, M., Brown, N. J., Salome, C., Berend, N., Marks, G. B., and King, G. G. (**2011**). "Procedures to improve the repeatability of forced oscillation measurements in school-aged children," Resp. Physiol. Neurobiol. **177**, 199–206.

Smith, J. R. (**1995**). "Phasing of harmonic components to optimize measured signal-to-noise ratios of transfer-functions," Meas. Sci. Technol. **6**, 1343–1348.

Smith, P. L., Wise, R. A., Gold, A. R., Schwartz, A. R., and Permutt, S. (**1998**). "Upper airway pressure-flow relationships in obstructive sleep apnea," J. App. Physiol. **64**, 789–795.

Stevens, K. N. (**2000**). *Acoustic Phonetics* (MIT Press, Cambridge, MA), pp. 437–440.

Sundberg, J., Scherer, R., Hess, M., Müller, F., and Granqvist, S. (**2013**). "Subglottal pressure oscillations accompanying phonation," J. Voice **27**, 411–421.

Titze, I. R. (**2008**). "Nonlinear source-filter coupling in phonation: Theory," J. Acoust. Soc. Am. **123**, 2733–2749.

Titze, I. R., Baken, R. J., Bozeman, K. W., Granqvist, S., Henrich, N., Herbst, C. T., Howard, D. M., Hunter, E. J., Kaelin, D., Kent, R. D., Kreiman, J., Kob, M., Löfqvist, A., McCoy, S., Miller, D. G., Noé, H., Ronald, C., Scherer, R. C., Smith, J. R., Story, B. H., Švec, J. G., Ternström, S., and Wolfe, J. (**2015**). "Toward a consensus on symbolic notation of harmonics, resonances, and formants in vocalization," J. Acoust. Soc. Am. **137**(5), 3005–3007.

Titze, I. R., Riede, T., and Popolo, P. (**2008**). "Nonlinear source-filter coupling in phonation: Vocal exercises," J. Acoust. Soc. Am. **123**, 1902–1905.

van den Berg, J. (**1960**). "An electrical analogue of the trachea, lungs and tissues," Acta Physiol. Pharmacol. Neerlandica. **9**, 361–385.

Wade, L., Hanna, N., Smith, J., and Wolfe, J. (**2017**). "The role of vocal tract and subglottal resonances in producing vocal instabilities," J. Acoust. Soc. Am. **141**, 1546–1559.

Weibel, E. R. (**1963**). *Geometry and Dimensions of Airways of Conductive and Transitory Zones* (Springer, Berlin, Heidelberg), pp. 110–135.

Wolfe, J., Almeida, A., Chen, J. M., George, D., Hanna, N., and Smith, J. (**2013**). "The player-wind instrument interaction," SMAC-2013, Stockholm, pp. 323–330.

Zañartu, M., Mehta, D. D., Ho, J. C., Wodicka, G. R., and Hillman R. E. (**2011**). "Observation and analysis of *in vivo* vocal fold tissue instabilities produced by nonlinear source-filter coupling: A case study," J. Acoust. Soc. Am. **129** 326–339.

Zhang, Z., Neubauer, J., and Berry, D. A. (**2006**). "The influence of subglottal acoustics on laboratory models of phonation," J. Acoust. Soc. Am. **120**, 1558–1569.